Int. J. Heat Mass Transfer. Vol. 33, No. 2, pp. 275–286, 1990
Printed in Great Britain

0017–9310/90 $3.00+0.00

Vertical tube air flows in the turbulent mixed convection regime calculated using a low-Reynolds-number $k \sim \varepsilon$ model

M. A. COTTON and J. D. JACKSON
Department of Engineering, University of Manchester, Manchester M13 9PL, U.K.

(*Received* 18 *January* 1989)

Abstract—Heat transfer to fluids flowing in vertical tubes under conditions of combined forced and free ('mixed') turbulent convection can exhibit marked departures from the case of purely forced convection. Significant impairment or enhancement of heat transfer can occur, depending upon flow orientation and the degree of buoyancy influence. A second important phenomenon arising in the ascending flow configuration is the occurrence of very long thermal-hydraulic development lengths. Calculations performed using a formulation of the Launder and Sharma low-Reynolds-number $k \sim \varepsilon$ turbulence model for developing flow in a tube show close agreement with a range of experimental heat transfer data and flow profile measurements for air, major discrepancies occurring only in strongly buoyancy-influenced descending flow.

1. INTRODUCTION

THE STUDY of convective heat transfer is commonly divided into the branches of forced convection (where motion is in response to an externally-applied pressure difference) and free convection (where motion is caused by a non-uniform distribution of gravitational body force arising from density variations within the fluid). Under conditions where both mechanisms operate simultaneously the heat transfer regime is termed 'mixed' or 'combined' convection. The present study is concerned with ascending and descending turbulent mixed convection flows in vertical tubes. These exhibit complex thermal-hydraulic behaviour, the most important external manifestation of which is gross impairment or enhancement of heat transfer. It is found that heat transfer in ascending flow may be impaired with respect to forced convection (at moderate heat loadings) or enhanced (at high heat loadings), whereas in descending flow heat transfer is enhanced throughout the turbulent mixed convection regime. An important feature of the ascending flow case is that development lengths of the order of 100 tube diameters are found to occur in the region of maximum heat transfer impairment. The impairment phenomenon is of particular practical importance in relation to post-trip heat removal from nuclear reactors and the occurrence of impaired and enhanced heat transfer has implications for all heat exchange equipment involving mixed convection in vertical passages.

The present contribution is part of a continuing programme of work [1, 2] in which the low-Reynolds-number two-equation ($k \sim \varepsilon$) turbulence model of Launder and Sharma [3] (a re-optimization of the Jones and Launder [4, 5] model) is applied to vertical tube flows in the turbulent mixed convection regime. All equations are cast in a formulation for developing flow. Extensive comparison is made against experimental measurements of heat transfer and flow profiles [6–10]. The working fluid used in the experiments was air (or nitrogen [8]) and the process of heat transfer in the mixed convection regime for the cases studied is not further complicated by significant temperature-dependent property variations (as may be the case where liquids such as water or oil or fluids at near-critical conditions are employed).

The selection of the low-Reynolds-number model was guided by consideration of the modifications that occur to the turbulent shear stress distribution, and thus shear production of turbulence, in the near-wall region of mixed convection flows (identified by Hall and Jackson [11]) and by the experience gained by other workers in applying simpler forms of turbulence closure to the problem. Abdelmeguid and Spalding [12] found that the high-Reynolds-number $k \sim \varepsilon$ model of Launder and Spalding [13] yielded the correct trends of impairment and enhancement in mixed convection heat transfer, however, no comparison with experimental heat transfer data was made. It was demonstrated by Walklate [14] that the use of a partial low-Reynolds-number treatment yielded more accurate results in the computation of the turbulent mixed convection data of Carr *et al.* [6] than did the parent high-Reynolds-number model. Renz and Bellinghausen [15] applied the Jones and Launder [4, 5] model to wall temperature data for an ascending flow of refrigerant near the thermodynamic critical point and found the correct qualitative trends of wall temperature development, although significant quantitative discrepancies were revealed. However, as indicated above, the highly variable properties at the conditions of such an experiment render this an especially stringent test of any model. Tanaka *et al.*

NOMENCLATURE

Bo buoyancy parameter, equation (16)
c_1 constant in $k \sim \varepsilon$ length scale, $\kappa/C_\mu^{0.75}$
c_p specific heat capacity at constant pressure
$C_{\varepsilon 1}, C_{\varepsilon 2}$ constants in production, sink terms of ε-equation
C_μ constant in constitutive equation of $k \sim \varepsilon$ model
D tube internal diameter
D_ε 'additional' dissipation term in k-equation
f_2 function in sink term of ε-equation
f_μ function in constitutive equation of $k \sim \varepsilon$ model
g magnitude of acceleration due to gravity
g_z component of acceleration due to gravity in z-direction
Gr_T Grashof number, $\beta g(T_w - T_b)D^3/\nu^2$
Gr Grashof number based on wall heat flux, $\beta g \dot{q} D^4/\lambda \nu^2$
k turbulent kinetic energy
Nu Nusselt number, $\dot{q}D/\lambda(T_w - T_b)$
Nu_0 Nusselt number for forced convection
p pressure
P rate of production of k
Pr Prandtl number, $c_p\mu/\lambda$
$\dot{q}$ wall heat flux
r, z radial, axial cylindrical polar coordinates
R tube internal radius
Re Reynolds number, $\rho W_b D/\mu$
Re_t turbulent Reynolds number
S_ε Yap dissipation source term
T temperature
T_0 reference temperature (upstream of the start of heating)
v, w velocity components in r, z-directions (fluctuating)
$\overline{vw}^+$ $\overline{vw}/(\tau_w/\rho)$
V, W velocity components in r, z-directions (time averaged)
W^+ $W/\sqrt{(\tau_w/\rho)}$
y normal distance from wall, $R-r$
y^+ $y\sqrt{(\tau_w/\rho)}/\nu$.

Greek symbols
β coefficient of volume expansion, $1/T_0$
ε rate of dissipation of k
$\tilde{\varepsilon}$ modified dissipation variable
κ von Karman constant
λ thermal conductivity
μ dynamic viscosity
ν kinematic viscosity, μ/ρ
ρ density corresponding to temperature T_0
ρ' fluctuating temperature-dependent density
σ_t turbulent Prandtl number
$\sigma_k, \sigma_\varepsilon$ turbulent Prandtl number for diffusion of k, ε
τ shear stress.

Subscripts
b bulk
CL centreline
g buoyant generation
t turbulent
w wall.

Superscripts
$\bar{}$ time averaged
$'$ fluctuating.

[16] compared a slight variant of the Jones and Launder model against their data for heated ascending flow of nitrogen and found generally good agreement between measured and calculated Nusselt number. Comparison with data was limited, however, and does not appear to include points in the vicinity of the condition of maximum heat transfer impairment. The fully-developed formulation used by Tanaka *et al.* is unsuitable for application to flows with long development lengths such as ascending turbulent mixed convection flows in the region of high heat transfer impairment. The reader interested in a detailed account of experimental and theoretical/numerical studies of turbulent mixed convection in vertical tubes is referred to a recent review [17]. In another recent work Launder [18] examines the application of turbulence models to a number of convective heat transfer problems including turbulent mixed convection flows.

Data for liquid metal mixed convection heat transfer are more sparse than those for air. In preparing the present paper the authors have restricted attention to well-documented air flows, however calculations for mercury and sodium are presented in ref. [19]. A comparison between experimental data for mixed convection heat transfer to water and numerical results is given in ref. [20].

2. MODEL FORMULATION

2.1. *Mean flow equations*

The mean flow equations are written in the 'thin shear' (or 'boundary layer') and Boussinesq approximations. Thus, in cylindrical polar coordinates the mean flow conservation equations are as follows:

continuity

$$\frac{1}{r}\frac{\partial(rV)}{\partial r} + \frac{\partial W}{\partial z} = 0; \tag{1}$$

momentum

$$\frac{1}{r}\frac{\partial}{\partial r}(\rho rVW)+\frac{\partial}{\partial z}(\rho W^2) = -\frac{dp}{dz} + \frac{1}{r}\frac{\partial}{\partial r}\left[r(\mu+\mu_t)\frac{\partial W}{\partial r}\right]+[1-\beta(T-T_0)]\rho g_z \quad (2)$$

where

$$g_z = \begin{cases} -g \text{ for ascending flow} \\ +g \text{ for descending flow} \end{cases};$$

energy

$$\frac{1}{r}\frac{\partial}{\partial r}(\rho rVT)+\frac{\partial}{\partial z}(\rho WT) = \frac{1}{r}\frac{\partial}{\partial r}\left[r\left(\frac{\mu}{Pr}+\frac{\mu_t}{\sigma_t}\right)\frac{\partial T}{\partial r}\right]. \quad (3)$$

2.2. *Turbulence model (Launder and Sharma) equations*

The present study employs the low-Reynolds-number $k \sim \varepsilon$ model of Launder and Sharma [3], a slight modification of the original model of this type due to Jones and Launder [4, 5]. The period since the publication of the original model has seen the development of a number of low-turbulent-Reynolds-number $k \sim \varepsilon$ formulations. Patel *et al.* [21] examined the performance of eight such models against data for external boundary layer flows and found that the Launder and Sharma model emerged as one of only three of these models to adequately reproduce the features of a flat plate boundary layer. Further examination indicated that the model continued to perform acceptably in the calculation of accelerated and decelerated flows. Henkes and Hoogendoorn [22] applied a number of $k \sim \varepsilon$ models to natural convection boundary layers and reached similar conclusions to those of Patel *et al.* Cast in cylindrical polar coordinates, the equations of the Launder and Sharma model are as follows:

constitutive equation

$$\mu_t = C_\mu f_\mu \frac{\rho k^2}{\hat{\varepsilon}}; \quad (4)$$

k-transport

$$\frac{1}{r}\frac{\partial}{\partial r}(\rho rVk)+\frac{\partial}{\partial z}(\rho Wk) = \mu_t\left(\frac{\partial W}{\partial r}\right)^2+P_g + \frac{1}{r}\frac{\partial}{\partial r}\left[r\left(\mu+\frac{\mu_t}{\sigma_k}\right)\frac{\partial k}{\partial r}\right]-\rho(\hat{\varepsilon}+D_\varepsilon) \quad (5)$$

where

$$P_g = \overline{\rho' w} g_z \quad (6)$$

$$D_\varepsilon = \begin{cases} 2\nu k/y^2 & (y^+ \leqslant 2) & (7a) \\ 2\nu(\partial k^{1/2}/\partial y)^2 & (y^+ > 2). & (7b) \end{cases}$$

Here $\hat{\varepsilon}$ is the modified dissipation variable to which the boundary condition $\hat{\varepsilon} = 0$ at $y = 0$ applies. The special form for D_ε adopted in the region $y^+ \leqslant 2$ is used because of convergence difficulties experienced when the standard form is retained in that region. Discussions have revealed that several users of low-Reynolds-number models have adopted equation (7a) for the region in the immediate vicinity of the wall. In alternative low-Reynolds-number $k \sim \varepsilon$ formulations the term is adopted for the entire flow [23].

$\hat{\varepsilon}$-Transport

$$\frac{1}{r}\frac{\partial}{\partial r}(\rho rV\hat{\varepsilon})+\frac{\partial}{\partial z}(\rho W\hat{\varepsilon}) = C_{\varepsilon 1}\frac{\hat{\varepsilon}}{k}\mu_t\left(\frac{\partial W}{\partial r}\right)^2+C_{\varepsilon 1}\frac{\hat{\varepsilon}}{k}P_g + \frac{1}{r}\frac{\partial}{\partial r}\left[r\left(\mu+\frac{\mu_t}{\sigma_\varepsilon}\right)\frac{\partial \hat{\varepsilon}}{\partial r}\right]-C_{\varepsilon 2}f_2\frac{\rho\hat{\varepsilon}^2}{k}+\frac{2\mu\mu_t}{\rho}\left(\frac{\partial^2 W}{\partial r^2}\right)^2. \quad (8)$$

Constants and functions

$$C_\mu = 0.09; \quad f_\mu = \exp(-3.4/[1+Re_t/50]^2);$$

$$Re_t = \frac{k^2}{\nu\hat{\varepsilon}}; \quad \sigma_k = 1.0; \quad \sigma_\varepsilon = 1.3; \quad C_{\varepsilon 1} = 1.44;$$

$$C_{\varepsilon 2} = 1.92; \quad f_2 = 1.0-0.3\exp(-Re_t^2). \quad (9)$$

Turbulent Prandtl number

$$\sigma_t = 0.9. \quad (10)$$

In a series of calculations where P_g was included, one of two modelling strategies was adopted. In both cases, the starting point was to re-cast equation (6) in terms of fluctuating temperature. Thus, in accordance with the Boussinesq approximation

$$P_g = -\beta\rho\overline{wT'}g_z. \quad (11)$$

The first approach to modelling the velocity–temperature correlation relies upon the concept of an isotropic turbulent thermal conductivity

$$\rho c_p\overline{wT'} = -\lambda_t\frac{\partial T}{\partial z} \quad (12)$$

where

$$\lambda_t = c_p\mu_t/\sigma_t. \quad (13)$$

Now, although λ_t is notionally isotropic, equations of the form of equation (12) are generally applied only to the turbulent heat flux in the direction of the principal temperature gradient (the radial direction) and may lead to a poor approximation to the turbulent heat flux in the axial direction. The 'generalized gradient diffusion hypothesis' (GGDH) of Daly and Harlow [24] may provide a better model for P_g. Within the framework of the GGDH the axial turbulent heat flux is related to the principal gradient direction

$$\overline{wT'} = -\frac{1}{C_{1T}}\frac{k}{\hat{\varepsilon}}\overline{vw}\frac{\partial T}{\partial r} \quad (14)$$

in which $C_{1T} = 3.2$. Tests reported in refs. [25, 26] have indicated that inclusion of P_g has a negligible effect when modelled in accordance with the isotropic turbulent thermal conductivity concept and only a second-order effect when modelled using the GGDH. Such results serve to reinforce the understanding that buoyancy effects in turbulent mixed convection vertical tube flows are primarily 'indirect' (acting upon shear production of turbulence) and that direct buoyant generation is of minor importance.

2.3. *Additional (Yap) dissipation source term*

The majority of the calculations reported below were executed using the formulation of equations (1)–(5) and (7)–(10) (with $P_g = 0$). In some descending flow (enhanced heat transfer) calculations, however, the effect of including an additional source of dissipation proposed by Yap [27] was investigated; for these cases a term S_ε is added to the right-hand side of equation (8)

$$S_\varepsilon = 0.83\left[\frac{k^{3/2}}{\hat{\varepsilon}c_1 y} - 1\right]\left[\frac{k^{3/2}}{\hat{\varepsilon}c_1 y}\right]^2 \frac{\rho\hat{\varepsilon}^2}{k} \qquad (15)$$

where $c_1 = 2.5$.

In the logarithmic region of a uniform shear stress boundary layer the length scale $k^{3/2}/\hat{\varepsilon}$ is equal to $c_1 y$ and S_ε is zero; as the length scale increases above the equilibrium value equation (15) provides an additional source of $\hat{\varepsilon}$ which itself acts to reduce the length scale and restrict the extent of departures from equilibrium values [18]. In the case of reduced length scales S_ε is a sink of dissipation, however in this event the quadratic term in equation (15) serves to limit the magnitude of the expression. The action of the Yap source term in turbulent mixed convection is examined in Section 3.1.

2.4. *Numerical procedures*

Discretization of the equation set is performed according to a finite volume/finite difference scheme following Leschziner [28] and the discretized equations are solved using a 'marching' solution procedure. Correction of the pressure gradient and axial velocity profile at each axial station in order to satisfy overall continuity is achieved using a method due to Raithby and Schneider [29]. The method possesses the dual merits of requiring only one additional solution of a discretized equation set and of producing exact values for the velocity set and dp/dz (cf. approximate methods in which terms are omitted from the discretized momentum equation to perform the correction).

An axial step length of approximately two viscous sublayer thicknesses (the sublayer for this purpose being taken to have a thickness corresponding to $y^+ = 5$) is employed. The radial grid consists of 101 nodes which are distributed to give a high concentration of grid lines near the wall (the wall-adjacent node is positioned at $y^+ \simeq 0.5$). Full details of the calculational procedures adopted and the sensitivity tests applied are given in ref. [25].

3. RESULTS AND DISCUSSION

Calculations have been performed using the Launder and Sharma [3] low-Reynolds-number $k \sim \varepsilon$ turbulence model as detailed in Sections 2.1 and 2.2; where the Yap [27] dissipation source term (Section 2.3) has been included this is stated explicitly. P_g is omitted from the formulation in all the calculations presented here.

3.1. *Heat transfer impairment and enhancement*

In an attempt to best illustrate the phenomena under consideration and also in order to link the present turbulence model calculations with the much simpler semi-empirical model of Hall and Jackson [11] the authors have adopted three different methods of presenting comparisons with experimental heat transfer data:

(a) Calculations at a single Reynolds number are compared against data obtained under a range of conditions by casting both computations and measurements in terms of a 'buoyancy parameter', Bo

$$Bo = 8\times10^4 \frac{Gr}{Re^{3.425}\,Pr^{0.8}}. \qquad (16)$$

The buoyancy parameter was developed by Hall and Jackson [11] from consideration of modified shear production of turbulent kinetic energy under mixed convection conditions. Equation (16) is the most recent form of the parameter to be developed (see ref. [17]); recourse to empirical flow resistance and forced convection heat transfer correlations leads to an expression for heat transfer impairment/enhancement

$$\frac{Nu}{Nu_0} = \left[1 \pm \frac{Bo}{(Nu/Nu_0)^2}\right]^{0.46} \qquad (17)$$

where the negative sign applies for ascending flow and the positive sign for descending flow.

Variants of equation (17) have found application in nuclear reactor heat transfer modelling [30].

(b) The second approach employed is to make direct case-by-case simulations of experimental tests and then to evaluate both data and calculations in terms of the buoyancy parameter, Bo (equation (16)). Thus a distinction should be drawn between the use of Bo on the one hand as the abscissa in Nu/Nu_0 vs Bo presentation of results and on the other hand the use of equation (17) which is an approximate formula for heat transfer impairment or enhancement.

(c) Finally, direct simulations of experimental tests are made and the results presented in terms of Nu vs Gr_T or Nu vs z/D.

Figure 1 shows comparisons of type (a) above. The trends of heat transfer impairment (with maximum impairment of over 50%) and enhancement discussed above are clearly evident. Present results obtained using the Launder and Sharma low-Reynolds-number $k \sim \varepsilon$ model are for $Re = 5000$ and $Pr = 0.7$. Bo is varied by increasing the Grashof number over the

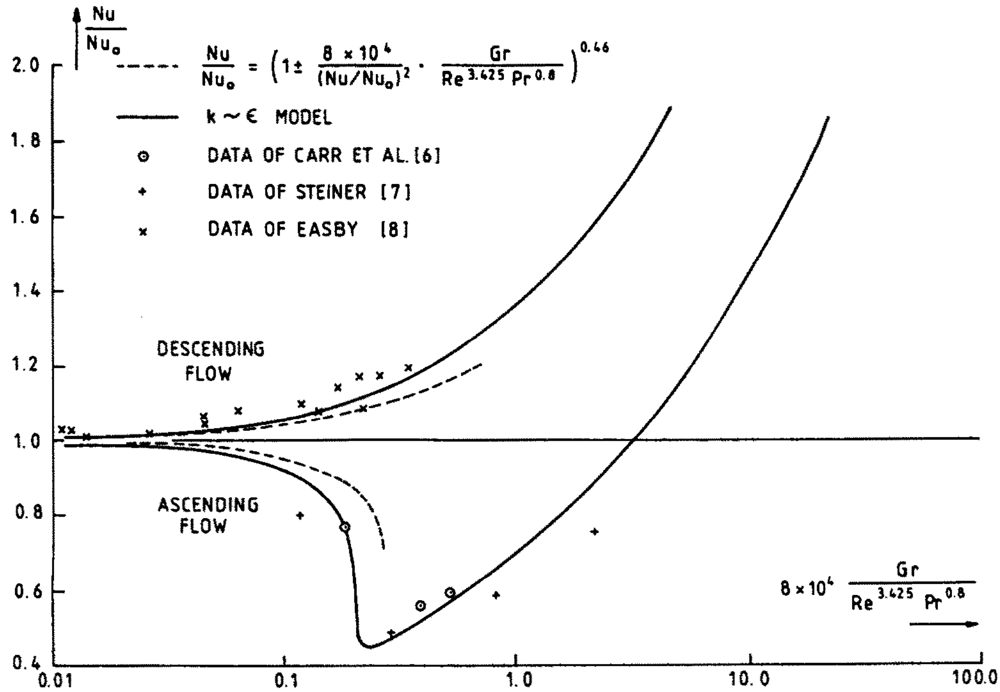

FIG. 1. Heat transfer impairment and enhancement in ascending and descending air flows.

range $4.4 \times 10^5 \leqslant Gr \leqslant 9.0 \times 10^8$ and Nusselt number is normalized to the computed value for fully-developed forced convection at the given Reynolds and Prandtl numbers. In the main, the points plotted for ascending flow represent Nusselt number at an axial position $z/D = 103.45$ (the location at which Carr *et al.* [6] made their measurements), although some points in the region of maximum impairment are for higher z/D (between $z/D = 106$ and 207) and there is evidence that, even at such high length-to-diameter ratios, a fully-developed condition has not been attained over the range $0.2 \leqslant Bo \leqslant 0.4$ (maximum impairment occurs at $Bo \simeq 0.22$). In the case of descending flow a fully-developed condition is attained by $z/D \simeq 30$. The experimental data shown on Fig. 1 were obtained under a range of conditions: Carr *et al.* [6] made measurements on air for $5000 \leqslant Re \leqslant 5400$ and $1.06 \times 10^7 \leqslant Gr \leqslant 2.22 \times 10^7$ at $z/D = 103.45$; the data of Steiner [7] are for air in the ranges $5000 \leqslant Re \leqslant 14900$ and $9.3 \times 10^7 \leqslant Gr \leqslant 2.17 \times 10^8$ at $z/D \simeq 60$ and Easby's [8] descending flow data are for nitrogen at $2100 \leqslant Re \leqslant 8300$, $1.4 \times 10^5 \leqslant Gr \leqslant 6.8 \times 10^6$ and $z/D \simeq 83$–150. In all cases Bo is evaluated at the experimental conditions quoted by the authors (taking $Pr = 0.7$ in the presentation of Steiner's and Easby's data) and the experimentally-determined Nusselt numbers are normalized with respect to the Dittus–Boelter equation

$$Nu_0 = 0.023 Re^{0.8} Pr^{0.4}. \tag{18}$$

The ascending flow data may be considered as a group since all are for large z/D and therefore fairly realistic comparison with the present results for $z/D \geqslant 103.45$ may be made. Two points emerge: firstly, agreement between present numerical results and the experimental data is acceptably close and, secondly, the buoyancy parameter, Bo, is seen to be a useful correlating parameter since the data are obtained over ranges of Re and Gr (although there is no test of the Pr-dependence of Bo). Unfortunately, none of the three sets of experimental data include measurements for fully-developed forced convection heat transfer and an uncertainty in the comparison is consequently introduced by the use of the Dittus–Boelter equation: this uncertainty may be quantified by the observation that computed Nu_0 at $Re = 5000$, $Pr = 0.7$ is 6.3% lower than that yielded by equation (18). It may be noted also that direct simulation of Runs N10, N12 and N13 of Carr *et al.* yielded discrepancies between computed values of Nusselt number and those obtained from the experimental measurements of 8, 12 and 11%, respectively (the computed values being lower).

A plot of the most recent form of the Hall and Jackson semi-empirical equation, equation (17), is also shown in Fig. 1. The equation captures the trends shown by both the present numerical results and the experimental data, although there are quantitative discrepancies.

The calculations shown in Fig. 2 are computed Nu/Nu_0 curves for ascending flow at $z/D = 10$, 20 and 50 ($Re = 5000$, $Pr = 0.7$) and the fully-developed

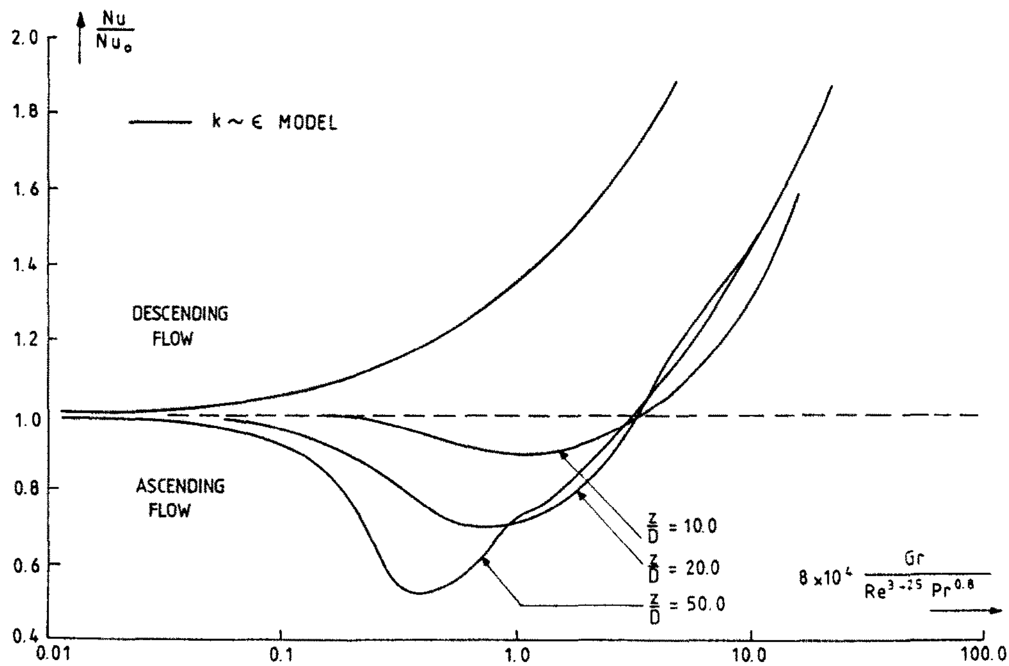

FIG. 2. Development effects in turbulent mixed convection.

descending flow curve reproduced from Fig. 1. The ascending flow curves demonstrate marked development effects. The distortions apparent in these curves arise in consequence of local recoveries in Nusselt number development, similar to those apparent in Fig. 5 (see below).

Byrne and Ejiogu [9] made measurements on heated ascending air flows with uniform wall temperature thermal boundary condition for $1.62 \times 10^4 \leqslant Re \leqslant 1.37 \times 10^5$ and $3.15 \times 10^{10} \leqslant Gr \leqslant 6.72 \times 10^{11}$ at low z/D, $z/D \simeq 5.5$. A comparison of type (b) above is made with the data (Fig. 3); computed Nu is normalized to computed Nu_0 and measured Nu is normalized to the Dittus–Boelter equation (taking $Pr = 0.7$). (Note: points may differ in location on the abscissa because $Gr = Gr_T\ Nu$ and thus Nu discrepancies enter the value of Gr.)

Figure 4 shows 'direct' (type (c)) comparison with the data of Axcell and Hall [10] for descending air flows under strong influence of buoyancy. The data were obtained at $z/D \simeq 5.5$, $Re \simeq 6 \times 10^4$ and $9.3 \times 10^8 \leqslant Gr_T \leqslant 2.7 \times 10^9$. It is seen that the 'standard' formulation of the turbulence model yields Nusselt number results that exhibit a discrepancy with

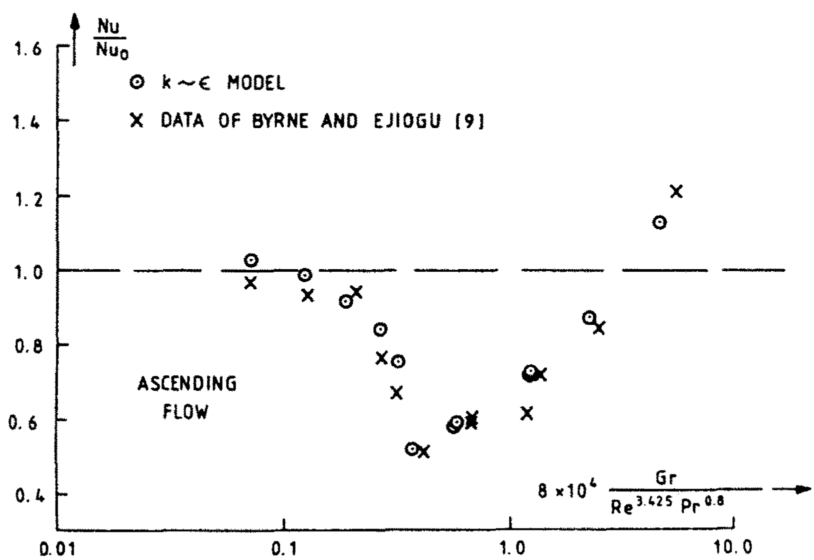

FIG. 3. Comparison with the ascending flow data of Byrne and Ejiogu [9].

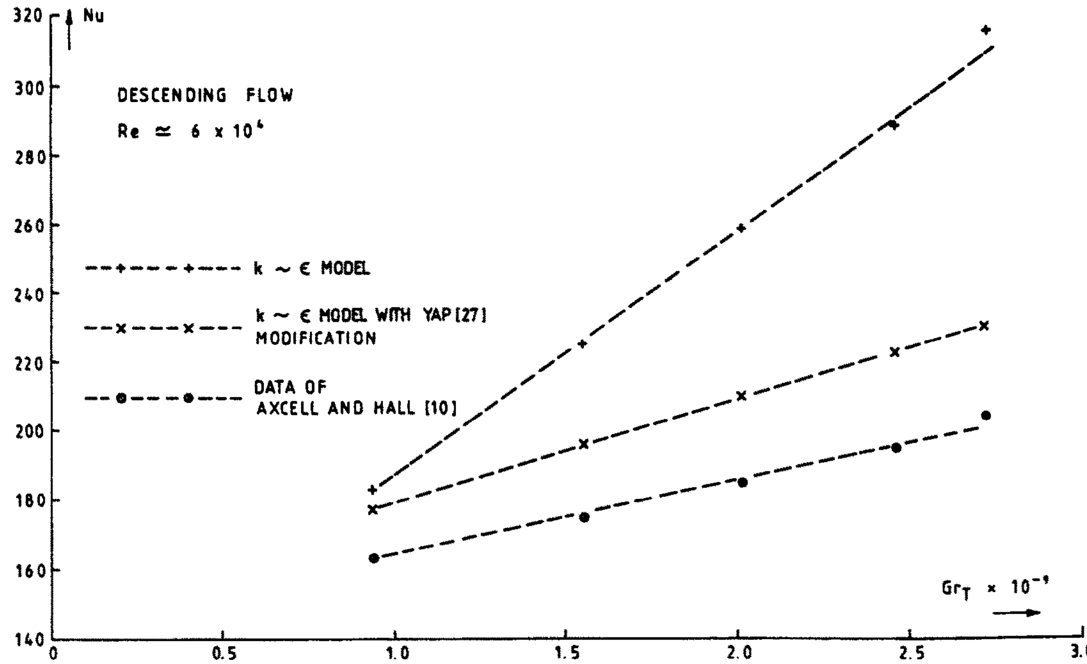

FIG. 4. Comparison with the descending flow data of Axcell and Hall [10]; inclusion of the Yap [27] source term.

respect to experiment which increases with Grashof number. Inclusion of the Yap dissipation source produces marked improvement in the degree of accord with data (Fig. 4). The action of the source term is to drive the turbulence length scale towards its equilibrium (uniform shear stress) value; without the additional term the turbulence model apparently yields the correct trends of behaviour in returning length scales that are increased in descending mixed convection, however the magnitude of the increase is too great. The formulation of equation (15) is such that S_ε has negligible effect in flows where turbulence levels are greatly reduced (a test on the ascending flow Run N13 of Carr *et al.* [6] showed that *Nu* changed by only 0.3% in response to inclusion of the term). Applications of the additional source term to other flows are discussed by Yap [27] and Launder [18]. Cotton [25] found that inclusion of buoyant production modelled according to the GGDH (with the Yap source omitted) served only to slightly increase computed Nusselt number at the highest Grashof number case of Fig. 4 (4.5% with respect to the standard formulation value of *Nu*).

The results of direct simulations (type (c) calculations) of Steiner's [7] experiments on ascending air flows are shown in Fig. 5. Unlike the other experimental data considered so far, Steiner reports measurements of Nusselt number development along the tube. Agreement between the computed values and experimental points is acceptably close for all four cases over the full axial extent of the measurements. (Note: in Ref. [7] Steiner does not mark z/D values on the axis, however, the text of the paper suggests that these values are as shown in Fig. 5.) It is interesting to observe the local recovery in Nusselt number occurring in the calculations and for which there is evidence in Steiner's data. Polyakov and Shindin [31] have recently published other measurements of *Nu* vs z/D in ascending turbulent mixed convection air flows and preliminary work to make comparison with these data is reported in ref. [26].

3.2. *Mean flow and turbulence profiles*

The remaining results to be presented are representative examples taken from a large number of simulations of experimental profile measurements.

Figure 6 shows the velocity profile measurements for Run N13 of Carr *et al.* [6] together with the present computed curve. The marked distortion of the profile measured by Carr *et al.* is captured to good accuracy by the model computations. Presentation of the same data in $W^+ - y^+$ coordinates (Fig. 7) serves to indicate the pronounced departure from near-wall 'universality' evident under conditions of turbulent mixed convection. Thus, any assumptions of universality made in order to construct wall functions for use with 'high-Reynolds-number' turbulence models applied to mixed convection are clearly highly questionable. Similarly close agreement with the velocity and temperature profiles measured by Steiner [7] is apparent in Fig. 8. Comparison with one of the velocity profiles

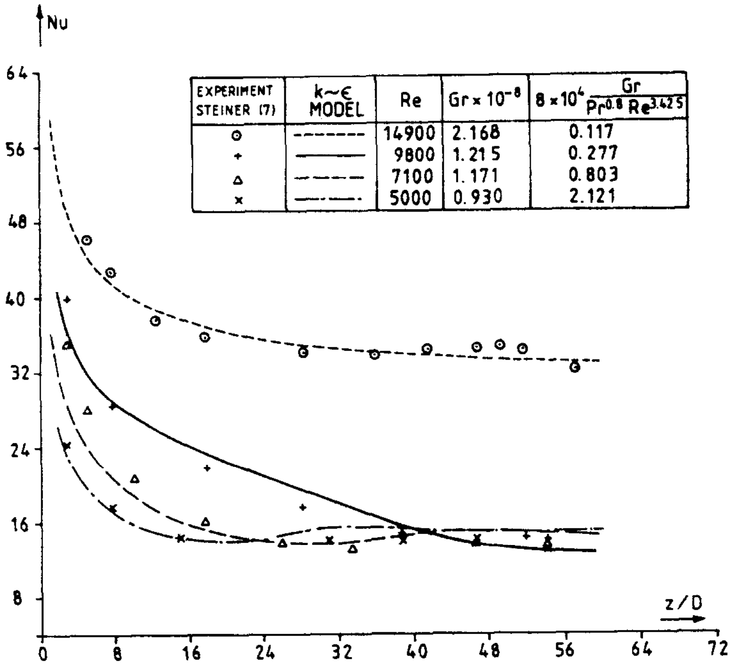

FIG. 5. Nusselt number development in ascending turbulent mixed convection: comparison with the data of Steiner [7].

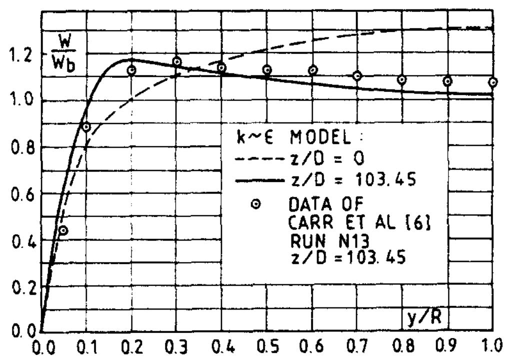

FIG. 6. Velocity profile in ascending flow: comparison with the data of Carr *et al.* [6], Run N13 (Re = 5000, $Gr = 2.22 \times 10^7$, z/D = 103.45).

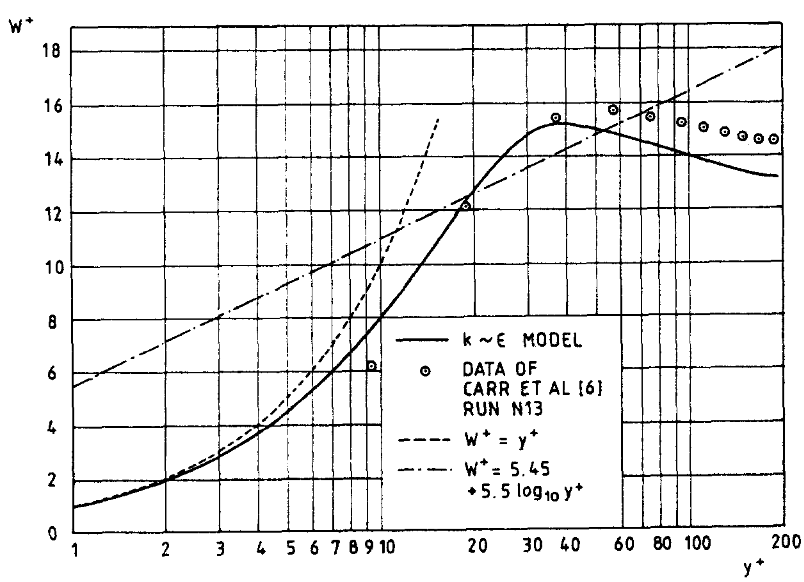

FIG. 7. Velocity profile of Fig. 6 plotted in 'universal' coordinates.

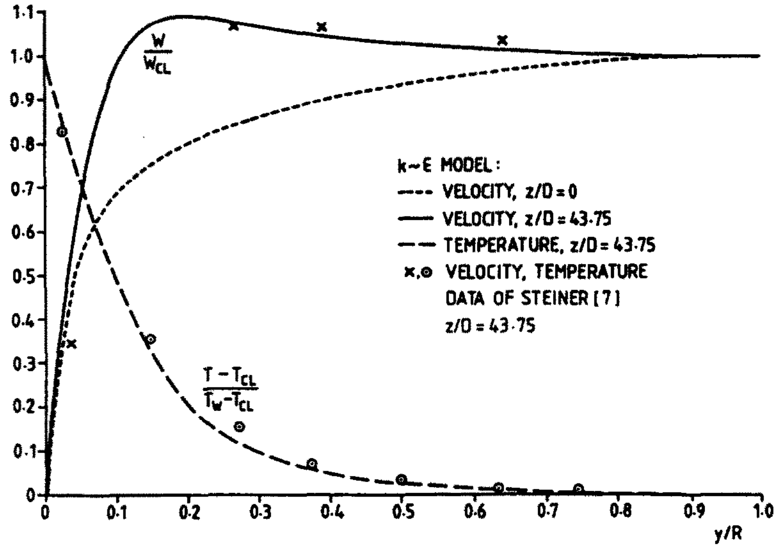

FIG. 8. Velocity and temperature profiles in ascending flow: comparison with the data of Steiner [7] ($Re = 9800$, $Gr = 1.215 \times 10^8$, $z/D = 43.75$).

measured by Axcell and Hall [10] in strongly-buoyancy-influenced descending flow is made in Fig. 9.

Figures 10 and 11 show comparisons between calculations and the Reynolds stress and turbulent heat flux data of Carr *et al.* [6]. There is some suggestion from Figs. 10 and 11 that the calculations yield too great a laminarization effect, however this observation must be tempered by the fact that the data are subject to some uncertainty because $\overline{vw}$ and $\overline{vT'}$ are deduced indirectly from measurements of the other terms of the momentum and energy equations assuming a fully-developed state (a condition not indicated by the calculations).

4. CONCLUSIONS

The low-Reynolds-number $k \sim \varepsilon$ turbulence model of Launder and Sharma [3] has been tested against experimental data for ascending [6, 7, 9] and descending [8, 10] turbulent mixed convection air flows. It is found that the model satisfactorily computes all these data with the exception of the descending flow data at high buoyancy influence obtained by Axcell and Hall [10]. Inclusion of an additional ε-equation source term proposed by Yap [27] improves agreement with the heat transfer data of ref. [10].

In the light of earlier studies and the work reported

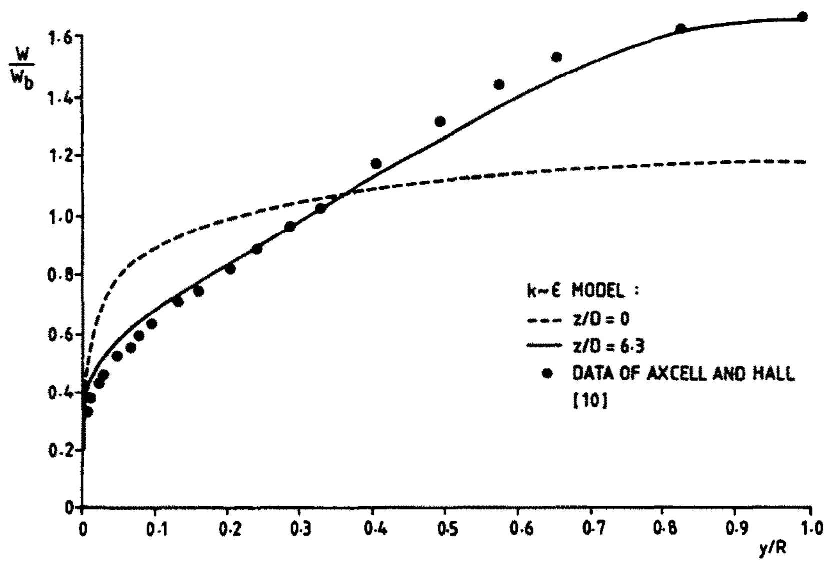

FIG. 9. Velocity profile in descending flow: comparison with the data of Axcell and Hall [10] ($Re = 6.07 \times 10^4$, $z/D = 6.3$, $Gr_T = 2.7 \times 10^9$ at this z/D).

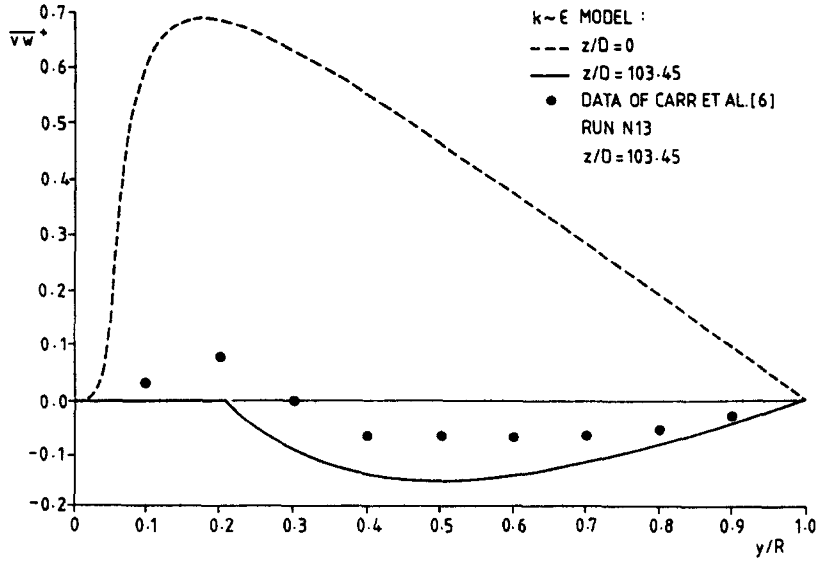

FIG. 10. Reynolds stress profile in ascending flow: comparison with the data of Carr *et al.* [6], Run N13.

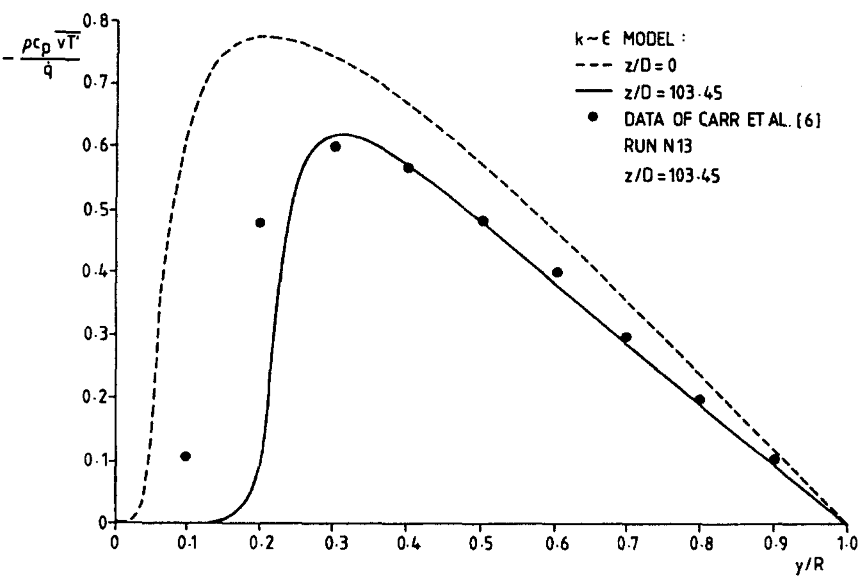

FIG. 11. Turbulent heat flux profile in ascending flow: comparison with the data of Carr *et al.* [6], Run N13.

here it is suggested that a low-Reynolds-number two-equation model represents the simplest formulation that may reasonably be expected to yield quantitatively accurate results for turbulent mixed convection flows. Furthermore, it is evident that the mean flow equations and the turbulence model must be cast in a developing flow framework in order to capture the complex thermo-fluid development behaviour found to occur in ascending flows.

Acknowledgements—The authors are grateful to Professor B. E. Launder for his encouragement and advice in the course of the present work and to Miss L. S. L. Yu for performing some of the computer runs used here.

REFERENCES

1. M. A. Cotton and J. D. Jackson, Calculation of turbulent mixed convection in a vertical tube using a low-Reynolds-number $k \sim \varepsilon$ turbulence model, *Proc. 6th Symp. on Turbulent Shear Flows*, Toulouse (1987).
2. M. A. Cotton and J. D. Jackson, Comparison between theory and experiment for turbulent flow of air in a vertical tube with interaction between free and forced convection. In *Mixed Convection Heat Transfer—1987* (Edited by V. Prasad, I. Catton and P. Cheng), ASME Publication HTD-Vol. 84 (1987).
3. B. E. Launder and B. I. Sharma, Application of the energy-dissipation model of turbulence to the calculation of flow near a spinning disc, *Lett. Heat Mass Transfer* 1, 131–138 (1974).

4. W. P. Jones and B. E. Launder, The prediction of laminarization with a two-equation model of turbulence, *Int. J. Heat Mass Transfer* **15**, 301–314 (1972).
5. W. P. Jones and B. E. Launder, The calculation of low-Reynolds-number phenomena with a two-equation model of turbulence, *Int. J. Heat Mass Transfer* **16**, 1119–1130 (1973).
6. A. D. Carr, M. A. Connor and H. O. Buhr, Velocity, temperature and turbulence measurements in air for pipe flow with combined free and forced convection, *J. Heat Transfer* **95**, 445–452 (1973).
7. A. Steiner, On the reverse transition of a turbulent flow under the action of buoyancy forces, *J. Fluid Mech.* **47**, 503–512 (1971).
8. J. P. Easby, The effect of buoyancy on flow and heat transfer for a gas passing down a vertical pipe at low turbulent Reynolds numbers, *Int. J. Heat Mass Transfer* **21**, 791–801 (1978).
9. J. E. Byrne and E. Ejiogu, Combined free and forced convection heat transfer in a vertical pipe, I.Mech.E. Symp. on Heat and Mass Transfer by Combined Forced and Natural Convection, Manchester, Paper C118/71 (1971).
10. B. P. Axcell and W. B. Hall, Mixed convection to air in a vertical pipe, *Proc. 6th Int. Heat Transfer Conf.*, Toronto, Paper MC-7 (1978).
11. W. B. Hall and J. D. Jackson, Laminarization of a turbulent pipe flow by buoyancy forces, ASME Paper 69-HT-55 (1969).
12. A. M. Abdelmeguid and D. B. Spalding, Turbulent flow and heat transfer in pipes with buoyancy effects, *J. Fluid Mech.* **94**, 383–400 (1979).
13. B. E. Launder and D. B. Spalding, The numerical computation of turbulent flows, *Comp. Meth. Appl. Mech. Engng* **3**, 269–289 (1974).
14. P. J. Walklate, A comparative study of theoretical models of turbulence for the numerical prediction of boundary layer flows, Ph.D. thesis, University of Manchester Institute of Science and Technology (1976).
15. U. Renz and R. Bellinghausen, Heat transfer in a vertical pipe at supercritical pressure, *Proc. 8th Int. Heat Transfer Conf.*, San Francisco, Paper IF-15 (1986).
16. H. Tanaka, S. Maruyama and S. Hatano, Combined forced and natural convection heat transfer for upward flow in a uniformly heated vertical pipe, *Int. J. Heat Mass Transfer* **30**, 165–175 (1987).
17. J. D. Jackson, M. A. Cotton and B. P. Axcell, Studies of mixed convection in vertical tubes, *Int. J. Heat Fluid Flow* **10**, 2–15 (1989).
18. B. E. Launder, On the computation of convective heat transfer in complex turbulent flows, *J. Heat Transfer* **110**, 1112–1128 (1988).
19. M. A. Cotton, J. D. Jackson and L. S. L. Yu, Application of a low-Reynolds-number two-equation turbulence model to mercury and sodium flows in the turbulent mixed convective regime, *Proc. 7th Symp. on Turbulent Shear Flows*, Stanford University (1989).
20. J. D. Jackson, M. A. Cotton, L. S. L. Yu and N. M. Rouai, Turbulent mixed convection heat transfer to water in a vertical tube—comparison between experiment and theory. Paper presented at Anglo-Soviet Seminar on Turbulent Convection, Institute for High Temperatures of the U.S.S.R. Academy of Sciences, Moscow (May 1989).
21. V. C. Patel, W. Rodi and G. Scheuerer, Turbulence models for near-wall and low-Reynolds-number flows: a review, *AIAA J.* **23**, 1308–1319 (1985).
22. R. A. W. M. Henkes and C. J. Hoogendoorn, Comparison of turbulence models for the natural convection boundary layer along a heated vertical plate, *Int. J. Heat Mass Transfer* **32**, 157–169 (1989).
23. K. Y. Chien, Predictions of channel and boundary-layer flows with a low-Reynolds-number turbulence model, *AIAA J.* **20**, 33–38 (1982).
24. B. J. Daly and F. H. Harlow, Transport equations in turbulence, *Physics Fluids* **13**, 2634–2649 (1970).
25. M. A. Cotton, Theoretical studies of mixed convection in vertical tubes, Ph.D. thesis, University of Manchester (1987).
26. M. A. Cotton and I. D. Nott, Computation of developing turbulent mixed convection heat transfer to air in a vertical tube: comparison of a low-Reynolds-number $k \sim \varepsilon$ model with recent experiments. Paper presented at Anglo-Soviet Seminar on Turbulent Convection, Institute for High Temperatures of the U.S.S.R. Academy of Sciences, Moscow (May 1989).
27. C. R. Yap, Turbulent heat and momentum transfer in recirculating and impinging flows, Ph.D. thesis, University of Manchester Institute of Science and Technology (1987).
28. M. A. Leschziner, An introduction and guide to the computer code PASSABLE, Report, University of Manchester Institute of Science and Tecnology (1982).
29. G. D. Raithby and G. E. Schneider, Numerical solution of problems in incompressible fluid flow: treatment of the velocity–pressure coupling, *Numer. Heat Transfer* **2**, 417–440 (1979).
30. G. F. Jackson, Heat transfer data, including impairment by buoyancy, for a CAGR fuel cluster in a Reynolds number range 10^3–10^6, *Proc. 1st U.K. National Conf. on Heat Transfer*, Paper 4.1 (1984).
31. A. F. Polyakov and S. A. Shindin, Development of turbulent heat transfer over the length of vertical tubes in the presence of mixed air convection, *Int. J. Heat Mass Transfer* **31**, 987–992 (1988).

ECOULEMENT D'AIR DANS UN TUBE VERTICAL, EN REGIME DE CONVECTION MIXTE TURBULENTE, CALCULE PAR UN MODELE k–ε A FAIBLE NOMBRE DE REYNOLDS

Résumé—Le transfert thermique pour des fluides s'écoulant dans des tubes verticaux sous des conditions de convection turbulente mixte peur révéler des écarts marqués à la convection forcée. Une diminution ou un accroissement sensible de transfert peut se produire, selon l'orientation de l'écoulement et le degré d'influence du flottement. Un phénomène important dans l'écoulement ascendant est la très grande longueur d'établissement thermique-hydraulique. Des calculs à partir d'une formulation du modèle de turbulence k–ε à faible nombre de Reynolds selon Launder et Sharma, pour le développement de l'écoulement, montre un accord étroit avec des données expérimentales de transfert de chaleur et de profils de vitesse dans l'air, les désaccords apparaissent seulement dans les écoulements descendants fortement influencés par le flottement.

LUFTSTRÖMUNGEN IN VERTIKALEN ROHREN BEI EINER MIT EINEM k–ε-MODELL BERECHNETEN MISCHKONVEKTION

Zusammenfassung—Der Wärmeübergang in vertikalen durchströmten Rohren bei kombinierter erzwungener und freier turbulenter (Misch-)Konvektion kann ausgeprägte Abweichungen zu dem Fall der reinen erzwungenen Konvektion aufweisen. Eine wesentliche Verschlechterung oder Verbesserung des Wärmeübergangs, abhängig von der Strömungsrichtung und dem Grad des Auftriebseinflusses, kann sich einstellen. Ein zweites wichtiges Phänomen, das in aufsteigender Strömung auftritt, ist das Zustandekommen von sehr langen thermisch-hydraulischen Einlauflängen. Berechnungen, die mit dem Ansatz des k–ε-Turbulenzmodells für kleine Reynolds-Zahlen von Launder und Sharma durchgeführt wurden, zeigen für die Rohreinlaufströmung eine gute Übereinstimmung mit experimentell in Luft ermittelten Ergebnissen für Wärmeübergang und Strömungsprofil. Größere Unterschiede treten nur in Strömungen auf, die stark vom Auftrieb dominert wurden.

РАСЧЕТ ТЕЧЕНИЙ ВОЗДУХА В ВЕРТИКАЛЬНЫХ ТРУБАХ В РЕЖИМЕ ТУРБУЛЕНТНОЙ СМЕШАННОЙ КОНВЕКЦИИ С ПОМОЩЬЮ НИЗКОРЕЙНОЛЬДСОВСКОЙ МОДЕЛИ k–ε

Аннотация—Теплоперенос к жидкостям, текущим в вертикальных трубах в условиях вынужденной и свободной (смешанной) турбулентной конвекции может значительно отличаться от случая чисто вынужденной конвекции. В зависимости от направления течения и степени влияния на него подъемной силы может происходить заметное ослабление или усиление теплопереноса. Вторым важным явлением при восходящем течении может быть большая протяженность теплового и гидравлического начальных участков. Расчет с использованием низкорейнольдсовской $k \sim \varepsilon$ модели турбулентности Лондера и Шармы для течения, развивающегося в трубе, обнаруживает хорошее соответствие между экспериментальными данными по теплопереносу и измерениями профилей скорости для воздуха; причем основные расхождения наблюдаются только при нисходящем течении с сильным влиянием на него подъемной силы.